Microstructural investigation of low-density carbon–carbon composites

I. J. DAVIES*, R. D. RAWLINGS
Department of Materials, Imperial College, London SW7 2BP, UK

The microstructure of low-density (0.13–0.64 $Mg\,m^{-3}$) carbon–carbon composites was investigated using optical microscopy, scanning electron microscopy and image analysis. All samples initially contained varying proportions of rayon precursor carbon fibres, recycled fibrous material and phenolic resin precursor matrix, and were manufactured utilizing a vacuum moulding technique. Some of the composites were densified using the chemical vapour deposition (CVD) of pyrolytic carbon. All the composites were shown to have a two-dimensional planar random microstructure, with a distinct layering effect being seen on the microscopic (and sometimes macroscopic) level. The degree of layering in the composites was quantified utilizing image analysis and was found to be most pronounced in samples containing no recycled material, and least pronounced in samples containing all of its fibrous constituent as recycled material. The composites were found to be very porous, the pores consisting of mainly interconnecting open pores (typically 65–85% of the sample volume). In non-CVD samples the fibrous material was held together by thin (< 5 μm) discrete "matrix bonds", with a few large (typically 100 μm × 200 μm × 800 μm) fibre bundles also existing within the structure. In the CVD-processed material the deposit coat on the fibres was of even thickness throughout the composite and joined together fibrous material that was not previously in contact.

1. Introduction

Carbon–carbon composites consist of carbon fibres embedded in a carbon matrix, and due to their unique mechanical and thermal properties, have applications as widely varying as brake discs and heart valves [1]. Although much work has been carried out on C–C composites (e.g. [2–10]), the vast majority has been concerned with higher-density composites in the approximate range 1.4 to 1.8 $Mg\,m^{-3}$, used mainly for their high specific strength. Work carried out on lower-density C–C composites, also known as carbon-bonded carbon fibre (CBCF) composites, with densities in the approximate range 0.1 to 0.5 $Mg\,m^{-3}$ [11–15], has been mostly concerned with their excellent thermal properties and there are very few structural data available on this type of low-density composite.

At present CBCF composites are mainly used as furnace linings, especially in high-tech applications, e.g. the growing of single crystals, where their high purity (> 99.9 wt % carbon content [16]) is of great significance. Greater demands are being placed on these materials when in service and in order to understand fully their properties and to develop the CBCF composites further, more information is required on the microstructure. It was therefore opportune to institute a microstructural investigation of these composites as a function of the processing conditions.

This paper reports the results of the investigation of the microstructure of low-density CBCF composites, some of which had been densified by the chemical vapour deposition (CVD) of pyrolytic carbon. The techniques employed were optical microscopy (OM), scanning electron microscopy (SEM) and image analysis (IA).

2. Experimental procedure
2.1. Production of CBCF composites
All the samples tested were manufactured by Calcarb Ltd. A summary of the production method is given below.

(i) Rayon fibres were cut into 1.8 mm lengths, carbonized in a nitrogen atmosphere at 950 °C and then de-agglomerated by being passed through a milling operation. This type of fibrous material was termed "virgin fibre". To reduce production costs, and as a means to increase the density of the non-CVD samples, recycled fibrous material, taken from excess machining operations of the finished composite and milled to an appropriate size, was also utilized in the production of these samples. This type of fibrous material was termed "reworked fibre".

(ii) Varying proportions of virgin fibre, reworked fibre and a phenolic resin (the matrix precursor) were added to a water-filled mould to form a slurry. The water was then extracted under vacuum, leaving the

component materials, which had by then formed the required shape, in the mould.

(iii) The artefact was dried in an oven for several days, and then heated to 950 °C in a nitrogen atmosphere to carbonize the phenolic resin.

(iv) After this, the artefact was heated to 2000 °C under a reduced atmosphere of argon, to allow the evolution of impurities from the composite.

(v) In the case of some of the samples, densification via CVD was undertaken at 1000–1100 °C under reduced pressure using methane as the precursor and nitrogen as the carrier [17].

Although all the samples within this report underwent a similar manufacturing route, the proportions of precursor materials and CVD treatment varied for each sample such that two main groups of samples could be identified:

(i) *Non-CVD samples* contained various percentages of their fibrous component as reworked (recycled) fibrous material. Density ranged from $0.13 \ \mathrm{Mg \, m^{-3}}$ for a sample containing no reworked fibres to $0.46 \ \mathrm{Mg \, m^{-3}}$ for a sample containing all of its fibrous material as reworked fibres.

(ii) *CVD samples* originally contained approximately 20 wt % matrix, 30 wt % virgin fibre and 50 wt % reworked fibre, and had an initial density of $0.17 \ \mathrm{Mg \, m^{-3}}$. They were then further densified by CVD of pyrolytic carbon for up to 550 h, resulting in a maximum density of $0.44 \ \mathrm{Mg \, m^{-3}}$.

2.2. Microscopy
Samples for OM were cold-mounted in clear resin and then polished first with SiC paper, graduating to diamond lapping fluids down to a 1 μm surface finish.

Some of the OM samples were also examined by SEM but most of the SEM was carried out on fracture surfaces from three-point bend tests. Unlike most other ceramics, the electrical conductivity of the samples was sufficient not to require gold-coating.

2.3. Image analysis
IA was used to investigate the microstructural anisotropy of the samples by determining the angular distribution of fibres in particular spatial planes of the specimens. For instance, the extreme case of complete microstructural isotropy would lead to a constant angular distribution of fibres within any plane of the specimen, whereas any degree of microstructural anisotropy would be expected to lead to a non-constant angular distribution of fibres within at least some of the planes of the sample.

The specimens were prepared as for OM and analysed using an Olympus CUE-2 image analyser linked to an optical microscope. Considerable manipulation of the image was necessary to remove noise and unwanted objects and to separate fibres that were touching (otherwise the analysis software would not have recognized individual fibres). The orientations of the fibres were resolved into 60 separate angular groups ranging from 0 to 180° in 3° intervals. For a given sample at least 50 images were analysed in order to obtain the fibre distribution histogram.

3. Results and discussion
3.1. Virgin and reworked fibre morphologies
Fig. 1 is a scanning electron micrograph of a virgin carbon fibre surrounded by a sheath of CVD pyrolytic carbon. It can be seen that the virgin carbon fibre has a diameter of approximately 7 μm and that it has a "crinkly" cross-section which is typical of carbon fibre produced from a rayon precursor, as opposed to a more circular cross-section for carbon fibres produced from pitch and polyacrylonitrile (PAN) fibres. Also worth mentioning is that the deposition layer appears to be of approximately equal depth around the fibre.

Fig. 2 is a scanning electron micrograph which shows that the virgin fibres have a large aspect ratio. This is not surprising as the rayon fibres were cut into 1800 μm length bundles during the manufacturing process (giving an initial aspect ratio of approximately 250).

Figs 3 and 4 are scanning electron micrographs of reworked fibrous material. From Fig. 3 it can be seen that the reworked fibrous material has a greatest dimension of approximately 500 μm. Also of note is that the larger agglomerates are platelet in shape with aspect ratios of approximately 10. The reworked fibrous agglomerates therefore have a much smaller aspect ratio than the individual virgin fibres.

An individual rework platelet can be seen at the centre of Fig. 4 with the diameter and thickness being
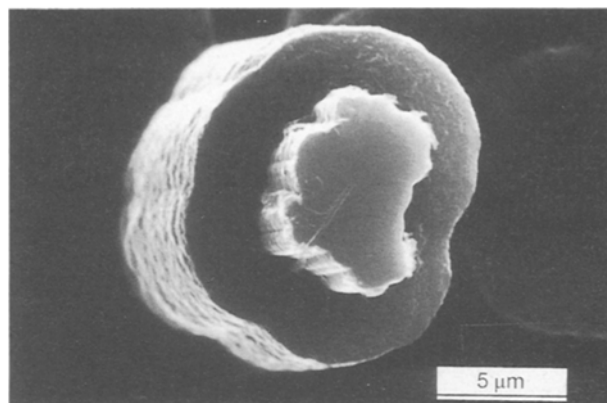

Figure 1 Scanning electron micrograph illustrating CVD pyrolytic carbon deposited on to a virgin carbon fibre.
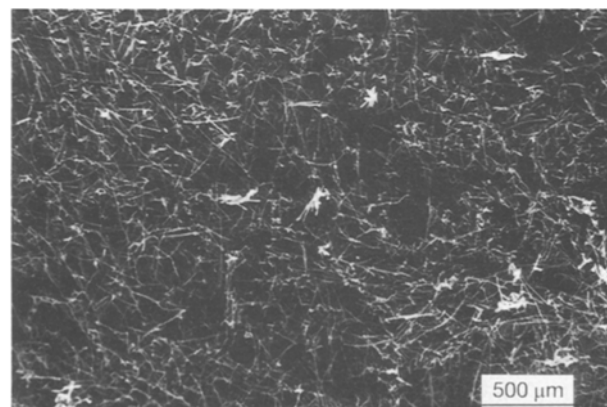

Figure 2 Scanning electron micrograph of a $0.17 \ \mathrm{Mg \, m^{-3}}$ non-CVD sample illustrating the large aspect ratio of virgin fibres.
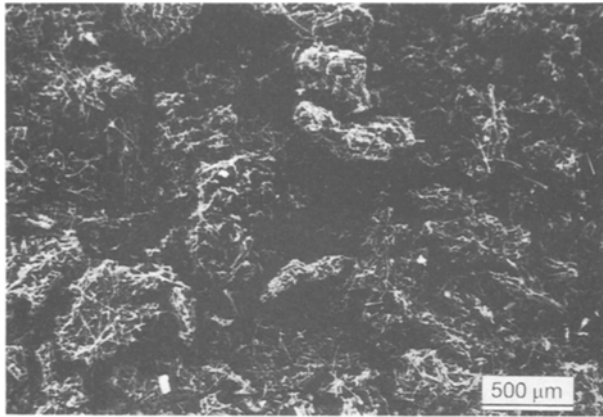
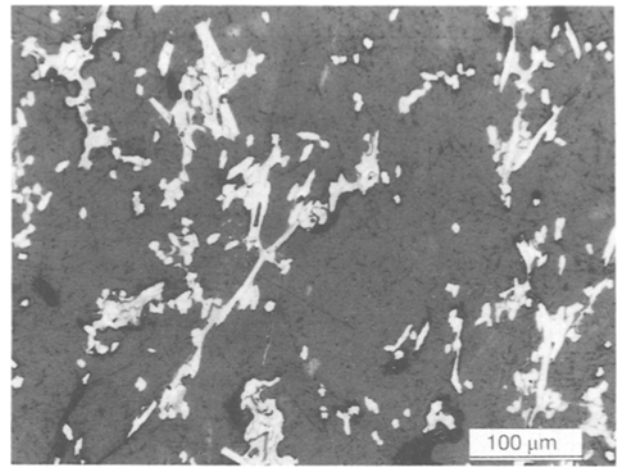*Figure 3* Scanning electron micrograph of reworked fibrous material.

Figure 5 Optical micrograph of a 0.17 Mg m^{-3} non-CVD sample.
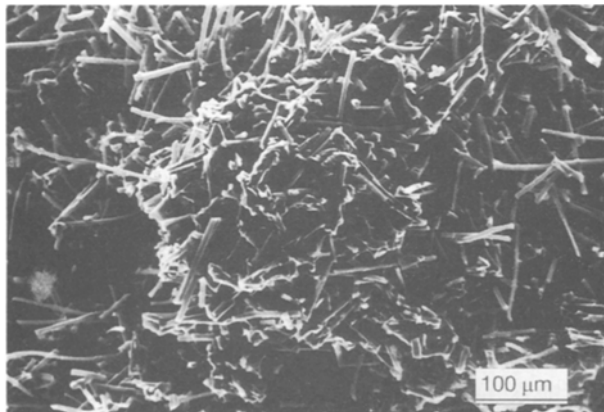

Figure 4 Scanning electron micrograph of a reworked agglomerate.

estimated at 350 and 50 μm, respectively. The rework particle agglomerates consist of small lengths of virgin fibre tightly packed, and appear to be denser than the composite as a whole (compare Figs 2 and 3).

3.2. Porosity and density
Fig. 5 is an optical micrograph of a 0.17 Mg m^{-3} non-CVD sample, with the lighter region being the fibrous and matrix components, and the darker regions being the porosity. From this micrograph it is obvious that the porosity content is exceptionally large, with typically 90 % of the volume of the composite being porosity in a 0.17 Mg m^{-3} sample, decreasing to 65 % porosity for a 0.50 Mg m^{-3} sample [18]. Also of note is that, due to the large proportion of porosity present, the pores themselves are of the open and interconnecting kind.

Table I gives the densities of a number of selected CBCF samples. The densities are extremely low due to the high porosity content. The densities vary by a factor of about 2.5 and are considered to depend on (i) the size, shape and proportions of the fibrous constituents, (ii) the extent of CVD, and (iii) the pressure under which the water was removed from the slurry in the moulding operation.

It is reasonable to assume that a smaller average particle size of a constituent would lead, if all other

parameters were fixed, to a greater packing density and thus a lower porosity fraction. This has been confirmed by the fact that using fibres of smaller length results in a sample of greater density and thus lower porosity, all other conditions being held constant [11].

Also, as shown earlier, compared with the virgin fibres, the reworked material has a lower aspect ratio (i.e. more spherical) and its greatest dimension is smaller. Thus a larger proportion of reworked material gives an increased packing density, as shown by the data in Table I.

Concerning the effect of CVD on the density of samples, it is generally found that the longer the duration of the CVD the greater is the density, though the rate of density increase with increasing CVD time would decrease once the open porosity fraction had been reduced enough to allow pore-blocking mechanisms [19, 20] to occur to a significant extent. For the samples tested within this report the initial open porosity fractions were so high that even after 550 h of CVD, the open porosity was enough so as to not significantly reduce the rate of increasing density [18]; the density increment was about 5×10^{-4} Mg m^{-3} h^{-1}.

It would also be expected that the density would depend on the water vacuum pressure in the manufacturing stage: the greater is the water vacuum pressure, the greater will be the packing density of the constituents. However, experiments have not been carried out to confirm this for these materials, though earlier researchers [11] have shown that using an increased forming pressure (analogous to water vacuum pressure) in the manufacture of similar composites did increase their density.

3.3. Fibre bundles
As shown in the micrographs of Fig. 6, large features (typically 100 μm × 200 μm × 800 μm) were sometimes present in the composites. These features consist of a large number of fibres that have been stuck together to form a fibre bundle.

It is suggested that these structures are due to rayon fibres sticking together upon carbonization, possibly

TABLE 1 Density of selected CBCF samples

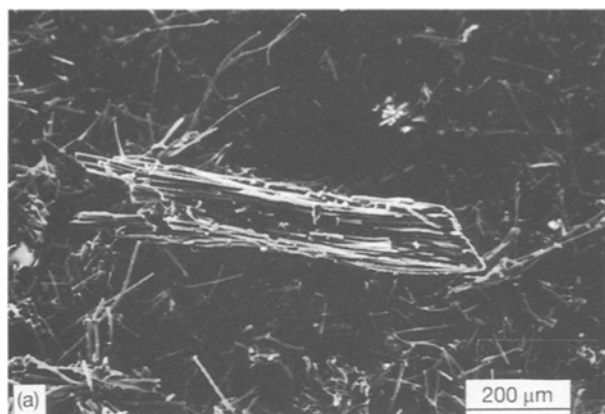| Sample	Virgin fibre (wt %)	Rework fibre (wt %)	Matrix (wt %)	CVD (wt %)	Density (Mg m^{-3})
Non-CVD with 0 % of fibre as rework	80	–	20	–	0.13
Non-CVD with 50 % of fibre as rework	40	40	20	–	0.15
Non-CVD with 100 % of fibre as rework	–	76	24	–	0.46
CVD before densification	32	48	20	–	0.18
CVD after 200 h densification	21	31	13	35	0.29
CVD after 550 h densification	13	20	8	59	0.44
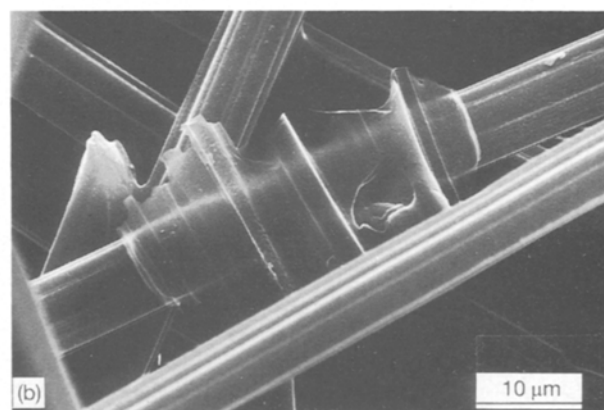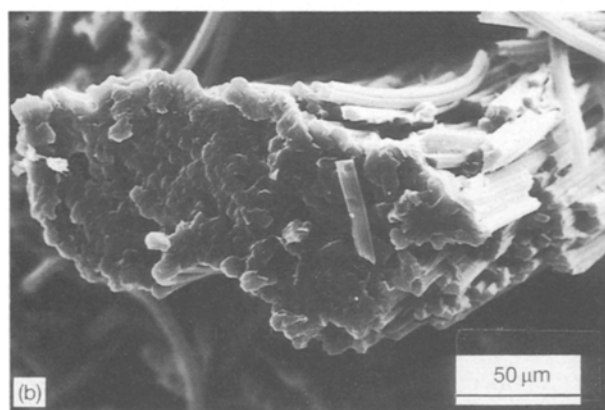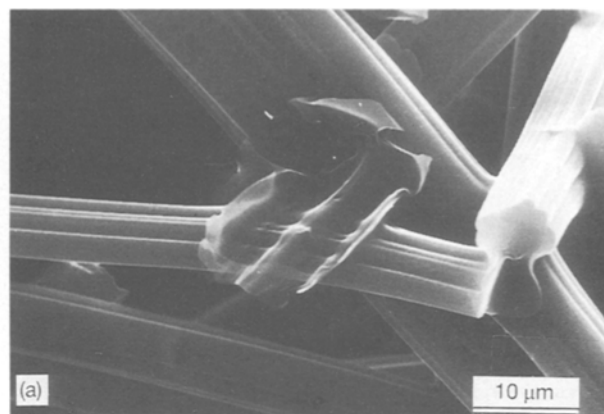
Figure 6 (a, b) Scanning electron micrographs of a fibre bundle.

Figure 7 (a, b) Scanning electron micrographs of a "discrete matrix bond".

because of the deposition of pyrolysed carbon caused by a heating rate that is too high [21]. This type of pyrolysed carbon is not the same as CVD pyrolytic carbon, but results from the gaseous by-products of fibre carbonization being deposited on to the surface of the fibres instead of being ejected from the reaction chamber. The fact that such bundles have also been seen in carbonized rayon fibres and in milled carbon fibres [18] is further evidence for this suggestion.

3.4. Fibre bonding

It was found that the phenolic resin matrix precursor did not coat itself evenly on the surface of the fibrous

material, but instead tended to accumulate at the junction where two fibres were touching each other (or else very nearly touching), so as to bridge the gap between the fibre surfaces. This type of bond is referred to as a "discrete matrix bond".

Fig. 7 illustrates fracture surfaces where one fibre has pulled away from another fibre, leaving clearly visible the discrete matrix bond that was previously holding the fibres together. From these micrographs it can be seen that (i) the bonds are discrete in nature, and (ii) the average thickness of the bonds is < 5 μm.

It is proposed that the discrete nature of the "matrix bonds" is due to the phenolic resin matrix precursor flowing along the characteristic ridges of the

341

carbonized rayon fibres and accumulating at the junctions between the fibres, thus forming a bridge between the fibres. This mechanism is shown schematically in Fig. 8 and the bridging of the resin at the junction of two fibres can be clearly seen in the micrograph of Fig. 9.

3.5. The CVD layer

Fig. 10a is an optical micrograph which illustrates the constituents present in a CVD sample. In this case, as well as the fibrous/matrix and porosity components being visible (the lightest and darkest areas, respectively), it can also be seen that the fibrous/matrix material is surrounded by another constituent. This constituent is the CVD layer, and it coats the composite to an even depth throughout, no doubt due to the large proportion of porosity of an open and interconnecting nature.

At higher magnification (Fig. 10b) it is just discernible that the CVD coating layer actually consists of two layers, an outer and an inner layer. An explanation for this is that the CVD process was not carried out in one continuous operation (i.e. it was carried out in stages), and thus the layering effect is thought to be due to the separate CVD stages having slight differences in operation conditions. It can also be seen from this figure that the CVD operation has joined together fibrous material that was not initially in contact, and this has been found to result in a stiffer and stronger material [22].
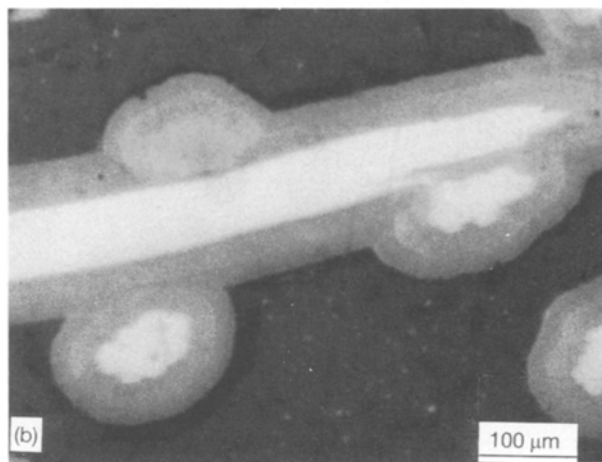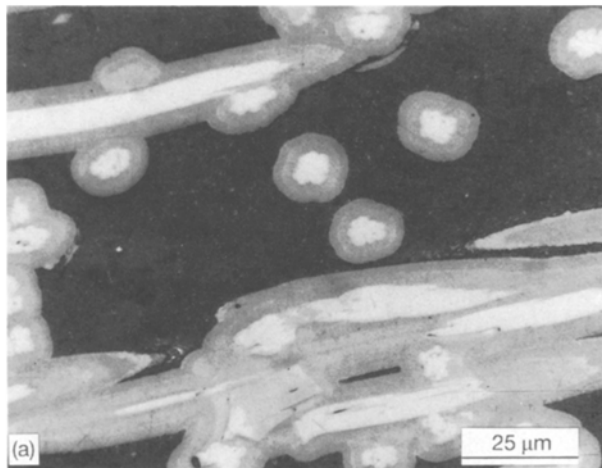

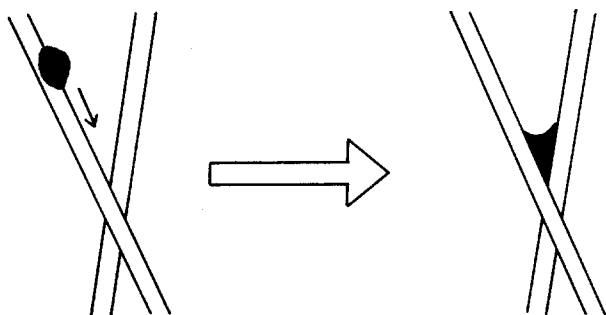*Figure 10* (a, b) Optical micrographs of a 0.44 Mg m^{-3} CVD specimen.

Figure 8 Schematic representation of resin matrix precursor flowing and bridging the gap between fibres.
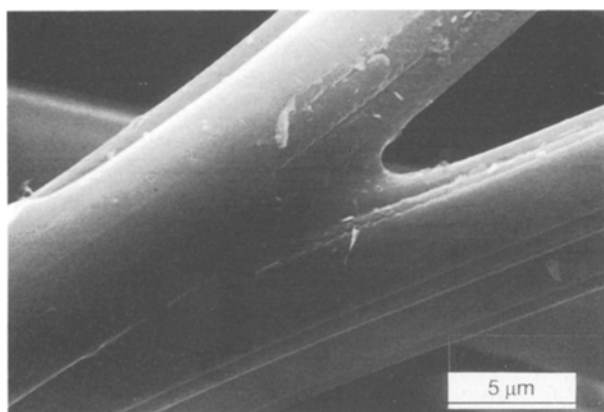
3.6. Anisotropy

As stated earlier, the composites were vacuum-moulded and it would therefore not seem unreasonable to assume that virgin fibres of such a high aspect ratio (approximately 250) might be orientated preferentially in the composite, i.e. with a degree of microstructural anisotropy.

Visual examination of low-density non-CVD samples revealed a markedly layered structure indicative of orientation of the virgin fibres. The layers were perpendicular to the direction of water flow in the moulding operation. In order to determine the orientation of the fibres within the composite, planes perpendicular to (designated xy) and parallel to (designated zx or zy) the direction of water flow were examined.

3.6.1. Scanning electron microscopy

Fig. 11a is a scanning electron micrograph of a zx (or zy) plane in a 0.17 Mg m^{-3} non-CVD sample, and it can be seen that the layers run from the bottom left to the top right of the micrograph. Fig. 11b shows the layering effect under a greater magnification. Three distinct vertical layers can be seen in Fig. 11b with approximate layer thickness values in the range 50 to 150 μm. It is interesting to note that the fibres are concentrated within these layers, with only a few fibres

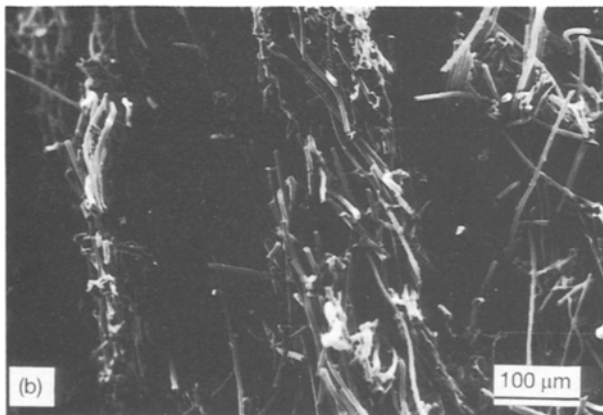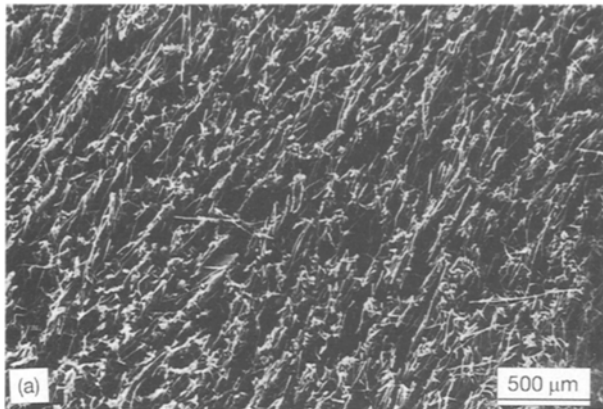*Figure 9* Scanning electron micrograph illustrating fibre bonding.

Figure 11 (a, b) Scanning electron micrographs illustrating the layering effect in the composite.

Figure 12 Schematic representation of a block of 2-D CBCF composite.

Figure 13 (a) Fibre orientation angle in (a) the xy plane and (b) the zx plane of a 0.13 Mg m^{-3} non-CVD specimen.

bridging the gap between the individual layers (i.e. many intralayer fibres but few interlayer fibres).

In contrast, scanning electron micrographs of xy planes indicate that there is no preferred orientation of the fibres, i.e. the fibres are arranged isotropically within the xy planes.

Thus it has been demonstrated that fibrous material was orientated preferentially with its major axis perpendicular to the direction of water flow in the vacuum moulding operation, resulting in what is commonly known as a two-dimensional (2-D) planar random structure. This structure is illustrated schematically in Fig. 12 along with axis designations.

3.6.2. Image analysis

Although the SEM studies showed that there was orientation of the fibres, the extent of the orientation was not quantified. Image analysis was used to determine the degree of orientation through orientation histograms. xy and zx planes of two samples were analysed; one of the specimens was a 0.13 Mg m^{-3} non-CVD sample containing no reworked fibre, and the other specimen was a 0.46 Mg m^{-3} non-CVD sample containing all of its fibrous material as reworked fibre.

Fig. 13a illustrates fibre orientation in the xy plane for the 0.13 Mg m^{-3} non-CVD sample, and although some scatter of the data is evident, the general trend indicates a fairly random variation of fibre number with angle. In contrast the orientation histogram for
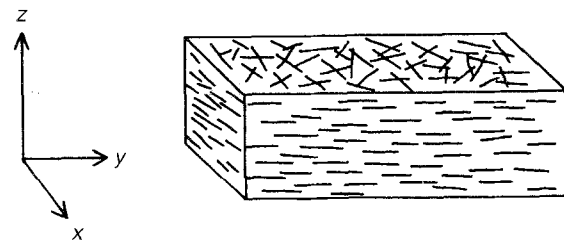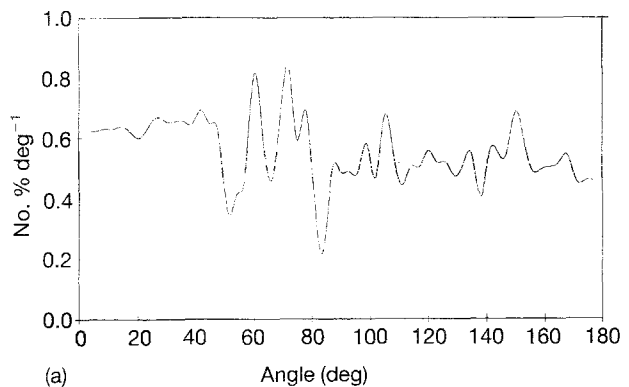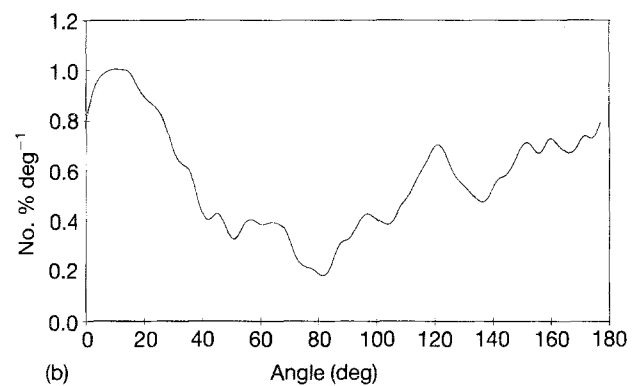
the zx (or zy) plane of the same sample (Fig. 13b) demonstrates marked anisotropy of the fibre orientations, there being a much smaller number of fibres orientated in the middle of the angle range when compared to low or high angles. This is further evidence for the 2-D random layer structure in the 0.13 Mg m^{-3} non-CVD sample.

The fibre orientation in the xy plane for the 0.46 Mg m^{-3} non-CVD sample (Fig. 14a) is similar to that for the 0.13 Mg m^{-3} sample. However, the orientation histogram for the zx (or zy) plane of the 0.46 Mg m^{-3} non-CVD sample (Fig. 14b) is significantly different to that previously discussed for the lower-density material. It can be seen that the fibre orientation is more random, i.e. the layering is less distinct, than in the 0.13 Mg m^{-3} non-CVD sample.

It is evident that the 0.13 Mg m^{-3} non-CVD sample is more anisotropic than the 0.46 Mg m^{-3} non-CVD sample, leading to the conclusion that the addition of reworked fibre to a composite reduces its microstructural anisotropy.

An explanation for this phenomenon is that, as shown earlier, the reworked particles are smaller in
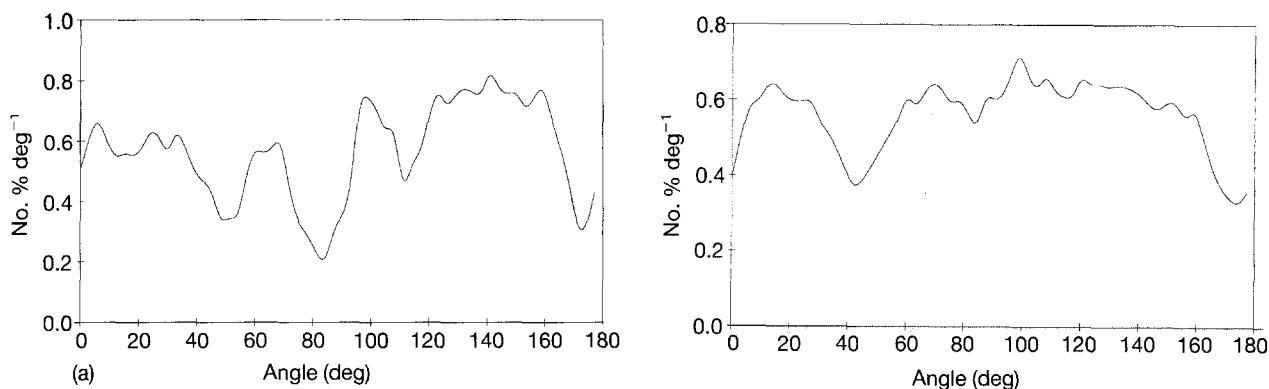
343

Figure 14 Fibre orientation angle in (a) the xy plane and (b) the zx plane of a 0.46 $Mg\,m^{-3}$ non-CVD specimen.

size, and have a smaller aspect ratio, than the virgin fibres, and so even though the actual rework particles are anisotropic in nature themselves, they are arranged near-randomly within the composite, thus reducing the microstructural anisotropy.

4. Conclusions
The following conclusions can be drawn:

(i) The composite consists of three components, namely fibres, matrix and recycled (reworked) material together with a large number of pores. The vast majority (typically 65–85 %) of the volume of the composite consists of interconnecting open pores.

(ii) The composite contains a small number of large features (typically 100 μm × 200 μm × 800 μm) which are probably due to rayon fibres within a bundle joining together upon carbonization.

(iii) In non-CVD samples the fibres and recycled material are bonded together by discrete, thin regions of the matrix (termed matrix bonds), as opposed to being surrounded by a continuous matrix as found in most composite systems. In CVD samples the CVD layer surrounds all the other components, and in some cases joins together fibres that were originally not in contact with one another.

(iv) A composite containing no reworked material (i.e. only virgin fibre and matrix) will be anisotropic due to the fibres (which have a large aspect ratio) being aligned perpendicular to the water flow during the vacuum-moulding stage of the manufacturing process. Thus the composite can be considered to consist of layers of planar random fibres, with each "layer" being bonded to its neighbour by a relatively small number of fibres/reworked material.

(v) A composite containing no fibres (i.e. only recycled material and matrix) will be the most isotropic. This is due to the low aspect-ratio reworked material being oriented more randomly when compared to higher aspect-ratio virgin fibre. This amounts to an anisotropic component being orientated in a near-random manner to give a relatively isotropic material.

Acknowledgements

References
1. E. FITZER, *Carbon* 25 (1987) 163.
2. T. G. GODFREY, D. L. McELROY and Z. L. ARDARY, *Nuclear Technol.* 22 (1974) 94.
3. M. MANOCHA, E. YASUDA, Y. TANABE and S. KIMURA, *Carbon* 25 (1988) 333.
4. O. SEH-MIN and L. JAI-YOUNG, *ibid.* 26 (1988) 769.
5. E. FITZER, W. HÜTTNER, and L. M. MANOCHA, *ibid.* 18 (1980) 291.
6. K. KOWBEL and C. H. SHAN, *ibid.* 28 (1990) 287.
7. S. SATO, A. KURUMADA, H. IWAKI and Y. KOMATSU, *ibid.* 27 (1989) 791.
8. C. R. THOMAS and E. J. WALKER, *High Temp. High Press.* 10 (1978) 79.
9. T. R. GUESS and W. R. HOOVER, *J. Compos. Mater.* 7 (1973) 2.
10. L. E. McALLISTER and W. L. LACHMAN, in "Handbook of Composites", Vol. 4, edited by A. Kelly (Elsevier Science, Amsterdam, 1983) p. 109.
11. C. D. REYNOLDS and Z. L. ARDARY, Report No. Y/DA-6925 (Union Carbide Corporation, Oak Ridge, Tennessee, 1976).
12. KUREHA F. R., Technical information F-4003, 84.01 (Kureha Chemical Industry Co. Ltd, Tokyo, 1984).
13. Product Data (Fiber Materials, Inc., Biddeford, Maine, 1987).
14. S. D. ELLACOTT, Report No. 9/004/02 (Calcarb Ltd, Bellshill, Strathclyde, UK, 1988).
15. G. C. WEI and J. M. ROBBINS, *Amer. Ceram. Soc. Bull.* 64 (1985) 691.
16. Report No. 1407 (Matcon, 13 Wolverton Avenue, Kingston-upon-Thames, Surrey, UK).
17. S. D. ELLACOTT, Calcarb Ltd, Bellshill, Strathclyde, UK, *Private Communication* (1992).
18. I. J. DAVIES, PhD thesis, University of London (1992).
19. W. V. KOTLENSKY, in "Chemistry and Physics of Carbon", Vol. 9, edited by P. L. Walker, and P. A. Thrower, (Dekker, New York, 1973) p. 173.
20. A. R. FORD, *Engineer* 224 (1967) 444.
21. R. BACON, in "Chemistry and Physics of Carbon", Vol. 9, edited by P. L. Walker, and P. A. Thrower (Dekker, New York, 1973) p. 2.
22. I. J. DAVIES and R. D. RAWLINGS, *to be published.*